17th World Conference on Earthquake Engineering, 17WCEE
Sendai, Japan - September 13th to 18th 2020

A COMPARISON OF VERTICAL RESPONSE SPECTRA FROM THE WESTERN CHINA WITH MODERN GROUND-MOTION PREDICTION EQUATIONS

Hao. Xing [1], John X. Zhao [2]

[1] *Ph.D. Candidate, Department of Geotechnical Engineering, School of Civil Engineering, Southwest Jiaotong University, xinghao0420@my.swjtu.edu.cn*

[2] *Professor, School of Civil Engineering, Shandong Jianzhu University, johnzhao1000@126.com*

Abstract

Vertical ground motions are very important for the design of bridges and buildings with long spans and many types of structures close to the surface fault ruptures. There have been relatively few studies on the vertical component for the strong motion records obtained in China compared with those on the horizontal components. Since the 2008 Wenchuan M_W 7.9 earthquake, a relatively large number of strong ground-motion records have been obtained in the western and the southwestern parts of China (WSC). In this manuscript, we present a comparison of the vertical response spectrum from the WSC region with five modern vertical ground-motion prediction equations (GMPEs), including the GMPEs by Bozorgnia and Campbell[1], Gülerce et al.[2], Stewart et al.[3], Çağnan et al.[4] (CAKS2017), and the GMPE for the shallow crustal and upper mantle earthquakes in Japan by Zhao et al.[5] (ZHAO2017). The dataset used in this study consists of 2403 strong-motion records from 449 events. 73 events were identified as mainshocks and 376 events were aftershocks. The data distribution with respect to magnitude is poor and many earthquakes have a small number of records. The maximum source distance was set to 300 km. To develop a GMPE based on this dataset only may not be feasible and a modeling guide presented in this manuscript may be useful. We built a correction function with magnitude, fault depth, source distance, and site terms. If the coefficient for a term in the correction function is zero or very small, the GMPE can be considered as the best model for this particular term. We find that all GMPEs underestimate the vertical response spectra of the WSC dataset for almost all spectral periods, except for CAKS2017 and ZHAO2017 models at a period range of 0.4-2.0s. The ZHAO2017 model has the best overall predictions and the between-event standard deviations vary between 0.27-0.38 on a natural logarithm scale after the correction functions are applied whereas the between-event standard deviations for the other four models vary between 0.33-0.65. In a period range of 0.15-1.0s, the linear magnitude scaling rates required by all GMPEs increase with increasing periods. The ZHAO2017 model describes the site effect well. We recommend that the ZHAO2017 can be used for the WSC dataset with or without modifications.

Keywords: Vertical component; ground-motion prediction equation; data comparative

1. Introduction

The western and southwestern parts of China (referred to as the SWC region hereafter) are one of the most earthquake-prone areas in China, especially in the western part of the Sichuan, Yunnan, the southern parts of Shaanxi and Shanxi Provinces. The Tibet Plateau and the Xinjiang Autonomous Region are also earthquake-prone areas. Numerous large and great earthquakes occurred in these regions. The 2008 Wenchuan earthquake with a moment magnitude (M_W) of 7.9, one of the most devastating events in the western part of Sichuan Province struck this region. A number of moderate and large earthquakes have occurred in the last 10 years in the SWC region, including the 2013 Lushan earthquake (M_W=6.6) in Sichuan Province, the 2014 Kangding earthquake (M_W=6.2) also in the Sichuan Province, and the 2014 Ludian earthquake (M_W=6.2) in the Yunnan Province. A large number of aftershocks also occurred following each large mainshock.

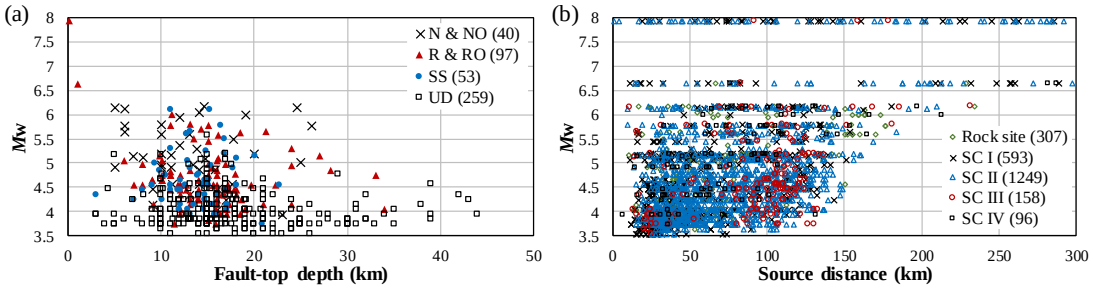

Figure 1 (a) The distribution of earthquakes with respect to fault depth and magnitude together with the number of events in different focal mechanism groups, and (b) the distribution of records with respect to source distance and magnitude together with the number of records in each site class.

We assembled a dataset from 449 events from the SWC region, referred to as the SWC dataset. Among these events, 190 earthquakes have focal mechanisms, 28 events have a normal (labeled by N), 12 have a normal-oblique (NO), 64 have a reverse (R), 33 have a reverse-oblique (RO), and 53 have strike-slip (SS) focal mechanisms. 259 events do not have a focal mechanism and are labeled as UD in Figure 1(a) together with the number of events with each focal mechanism type. The moment magnitudes for some events were from the Global CMT catalog if available and the others were estimated by using a correlation relationship between the calibrated moment magnitude and surface wave magnitude issued by the seismological agency in China. Among these events, only 73 were identified as the mainshocks according to the identification criterion from Wooddell and Abrahamson [6], with 677 records being from the mainshocks. Although a reasonably large number of strong-motion records from a large number of earthquakes are available for this study, the distributions of events and records are not ideal. There is a large magnitude gap in the dataset; for example, there is only one event between M_W 6.3 and M_W 7.8.

We used V_{S30}, the travel-time averaged shear-wave velocity of the top 30m soil as the site parameter for the Next Generation of Attenuation model (NGA)-West2 models whereas a site-period based site class was used as the site effect proxy for the Zhao et al. [7] model. Site class (SC) I sites have a site period of T_S <0.2s, SC II sites have a period range of 0.2s≤T_S <0.4s, SC III sites have a period range of 0.4s≤T_S <0.6s and SC IV sites have a site period of $T_S \geq$ 0.6s. In the SWC dataset, the stations with a measured shear-velocity profile are few and V_{S30} for many recording stations based on the limited measured shear-wave velocity profiles. Site classes for the other sites were derived from H/V ratios for most stations using the Zhao et al. (2006) method.

The dataset used in this study were recorded by 390 recording stations. 97 were assigned as SC I sites, 113 as SC II sites, 27 as SC III sites, 40 as SC IV sites, and 113 as rock sites that were combined into SC I sites for the model by Zhao et al. [5]. We used 2403 strong-motion records for PGA from 449 earthquakes and the distribution of records with respect to source distance and magnitude is presented in Figure 1(b) together with the numbers of records in each site class. For PGA, 900 records are from SC I sites, 1249 records from SC II sites, 158 records from SC III sites, and 96 records from SC IV sites. Among these stations 177 stations have only one record, 130 stations have four or fewer records, 52 stations have 5-19, and 31 stations have 20 or more records. The average number of records from each site is relatively small. At long periods, the numbers

of earthquakes and records decrease with increasing spectral periods. The limitations and shortcomings of the SWC dataset make it not possible to develop a robust GMPE without using some supplement data or using a function form of the GMPE developed by using a much larger dataset that has good distributions with all the important strong-motion modeling parameters. In this study, we will compare the SWC data with five modern GMPEs so as to provide a guide for developing a GMPE based on the SWC dataset or for selecting a GMPE for the SWC region to be used without modifications. Numerous studies compare the strong ground-motion records from one region with the GMPEs developed for another region for the purpose of calibrating a GMPE or identifying the differences in various physical ground motion parameters. For example, Lan et al. [8] compared the horizontal ground motions with the dataset used here with two NGA-West models (Abrahamson and Silva [9], Chiou and Youngs [10]) and two NGA-West2 models (Abrahamson et al. [11], and Chiou and Youngs [12]) and the Zhao et al. [7] model for the shallow crustal and upper mantle earthquakes in Japan. Lan et al. [8] concluded that the Zhao et al. [7] model was the best for the response spectra of the horizontal ground motions. Lan et al. [8] also suggested that it was necessary to use the aftershock in their study for the SWC region in order to evaluate the site and path effects properly for the horizontal component. However, the modeling of records from aftershocks did not make a significant improvement.

We will compare the ground motions with five GMPEs for the vertical ground motions, including those by Bozorgnia and Campbell [1] (BC2016), Çağnan et al. [4] (CAKS2017), Gülerce et al. [2] (GKAS2017), Stewart et al. [3] (SBSA2016), and Zhao et al. [5] (ZHAO2017). The BC2016, GKAS2017, and SBSA2016 GMPEs were all derived from the NGA-West2 dataset but the selections of records may vary from one model to another, especially for records outside of California. The CAKS2017 model was based on the records from Europe and the Middle East. Except for the BC2016 model all the other four models used aftershock data and only the GKAS2017 model has an aftershock term. The ZHAO2017 model has a positive constant for normal faulting events that occurred in a relatively small region in Japan. For some of the NGA-West or NGA-West2 GMPEs, the normal faulting events usually have a small negative constant term for short periods up to 0.5s. We assume that this normal event term of the ZHAO2017 model is not applicable to the SWC dataset and this term was set as zero in this study, with this model being referred to as ZHAO2017N. This assumption improved the maximum likelihood from the regression results at short periods after a statistical test was carried out without this term.

The magnitude and the distance ranges for the SBSA2016 model are the same as those for the BC2016 model. The BC2016, GKAS2017, and the ZHAO2017 models used the rupture distance when a fault plane is available and hypocentral distances for other events. The SBSA2016 model uses R_{JB} as the distance measure, i.e. the closest distance to the surface projection when a fault model is available and the epicentral distance for other earthquakes. V_{S30} was used as the site proxy parameter by all NGA models. NGA-West2 models used a very small number of strong-motion records from the SWC region in China to estimate the anelastic attenuation term and this term is referred to as the term for China. This reference of the China term is somewhat misleading as the records used in the NGA-West2 are from a very small part of the SWC region and Q values vary significantly in the different areas in this part of China.

2. Correction functions

In this study, we designed a set of correction functions with all terms based on the source, path and site effects. Firstly, the total residuals were computed and then separated into a constant term, between-event, and within-event parts by using a random effects model,

$$\xi_{i,j}^{T} = \xi_{i,j} + \eta_i + c \qquad (1)$$

$$\ln\left(y_{i,j}^{M}\right) = \ln\left(y_{i,j}\right) + c + \xi_{i,j} + \eta_i \qquad (2)$$

in which $\xi_{i,j}^{T}$ is the total residual for the j^{th} record from the i^{th} earthquake, $\xi_{i,j}$ is the within-event residual that has a zero mean and a standard deviation of σ, and η_i denotes the between-event residuals for the i^{th} event that has a zero mean and a between-event standard deviation of τ. Constant c is a correction term leading to that η_i and $\xi_{i,j}$ have a zero mean so that correction factors for the other term can be estimated. Symbol $y_{i,j}$ stands for

the predicted response spectrum by a GMPE and $y_{i,j}^{M}$ is the predicted spectrum corrected by exp(c). Equation (2) is referred to as the average-corrected GMPE. The maximum log-likelihood (MLL), and the standard deviations σ and τ from the decomposition in Equation (1) can be used as the goodness-of-fit parameters for the GMPEs compared here.

The correction term c reflects the overall goodness of fit, and if the constant term is not statistically significant this GMPE can be considered to fit the dataset very well on average. In theory, the constant c does not contain information of misfit to the source, path, and site effect if the dataset has an ideal distribution with respect to these ground motion parameters, as assumed in this study.

We designed the following correction function for the magnitude effect,

$$f_m(m_i) = a_1 + a_2\delta_N + a_3\delta_R + a_4\delta_{SS} + \begin{cases} b_1 m_i + b_2(m_i - m_{sc})^2 & \text{if } m_i \le m_c \\ b_1 m_i + b_2(m_c - m_{sc})^2 + b_3(m_i - m_c) & \text{if } m_i > m_c \end{cases} \quad (3)$$

in which a_1 is a constant, a_2, a_3, and a_4 are the added focal mechanism correction constants for three focal mechanism groups. The subscripts N, R, and SS for δ denote the normal and normal-oblique, reverse and reverse-oblique, and strike-slip focal mechanism groups, respectively. The effect of focal mechanisms is relative to the events that do not have a focal mechanism. The dummy variable δ has a value of 0.0 or 1.0, for example, δ_N has a value of 1.0 for the normal or normal oblique event and 0.0 for the events with the other focal mechanisms. Symbols b_1, b_2, and b_3 are the correction coefficients for the magnitude terms. Symbol m_i denotes the moment magnitude for the i^{th} event, and m_c and m_{sc} are magnitude constants and m_{sc}=6.3 and m_c=7.1 were used. The magnitude constant m_{sc} is not an independent regression coefficient and m_c is from the Zhao et al. [5] studies. The use of m_c=7.1 partially exclude the effect of the magnitude gap in our dataset, because the magnitude scaling rate for events in a magnitude range up to M_W=7.1 can be largely extrapolated from the events in a magnitude range of 3.5-6.6 and the magnitude scaling rate for events with M_W>7.1 will be constrained by the continuous magnitude scaling function and the records from the 2008 Wenchuan mainshock. The following correction function was designed for the depth effect,

$$f_h(h_i) = \begin{cases} d_1 h_i & \text{if } h_i \le h_c \\ d_1 h_c + d_2(h_i - h_c) & \text{if } h_i > h_c \end{cases} \quad (4)$$

in which h_i denotes the fault-top depth for the i^{th} event, h_c =25km is a depth constant, and d_1 and d_2 are the correction coefficients for the depth effect. All correction coefficients can be derived from the following function by regression analysis,

$$\eta_i = f_m(m_i) + f_h(h_i) + \gamma_i \quad (5)$$

in which γ_i is the residual that has a zero mean and a standard deviation of τ_N after adding the terms in Equations (2) and (3) to the corresponding GMPE. The standard deviation τ_N is referred to as the between-event standard deviation for the average-corrected GMPE $y_{i,j}^{M}$ in Equation (2) and can be used as a goodness-of-fit parameter for each average-corrected GMPE. The use of constant c in Equation (1) allows for that all regression variables in Equations (2) and (3) to represent the source terms and can be derived by a simple fixed effects regression analysis.

The following equation was used to decompose the within-event residuals $\xi_{i,j}$ of the j^{th} record from the i^{th} event into within-site and between-site components,

$$\xi_{i,j} = e_1 + e_2 ln(T_{VS30k}) + e_3 x_{i,j,k} + e_4 ln(r_{i,j,k}) + \lambda_{i,j} + \theta_k \quad (6)$$

$$r_{i,j} = x_{cro} + x_{i,j} + \exp(c_1 + c_2 C_m) \quad (7)$$

$$C_m = \begin{cases} m_i & if\ m_i \le C_{max} \\ C_{max} & if\ m_i > C_{max} \end{cases} \quad (8)$$

in which $x_{i,j}$ is the source distance for the j^{th} record from the i^{th} event, and T_{VS30}=120/V_{S30} with V_{S30} having a unit of m/s. T_{VS30} is a pseudo-site period and equals the site period if the bedrock depth is 30m. Subscript k denotes the k^{th} site. Symbol e_1 is a regression constant, e_2 denotes the added site term, e_3 denotes the added anelastic attenuation rate and e_4 stands for the added geometric attenuation rate. Variable x_{cro} is the added distance to avoid over magnitude saturation, i.e. to avoid the spectrum decreasing with increasing magnitude at source when $x_{i,j}$=0.0, The coefficient c_1, c_2, and C_{max}=7.1 are from Zhao et al. [5]. Symbol $\lambda_{i,j}$ denotes the within-site residuals that have a zero mean and a standard deviation of σ_{NS} which indicates how well the model could be improved when the distance terms in Equation (6) are added to the corresponding GMPE. Symbol θ_k denotes the between-site residuals having a zero mean and a between-site standard deviation of τ_{NS} that indicates how well the site modeling of the SWC dataset by a given GMPE plus the correction functions. Standard deviation σ_{NS} is referred to as the within-site standard deviation for the average-correct model denoted by $\ln(y_{i,j}^{M})$ in Equation (2). The separation of total residuals in Equation (2) and the use of constant c in Equation (1) allows that all regression variables in Equation (5) represent the path and the site terms and can be derived by a random effects regression analysis.

3. Maximum log-likelihood and correction coefficients

Next, we present the maximum log-likelihood from Equation (2), the constant correction term c, and the correction coefficients from Equations (2) and (3) for each GMPE.

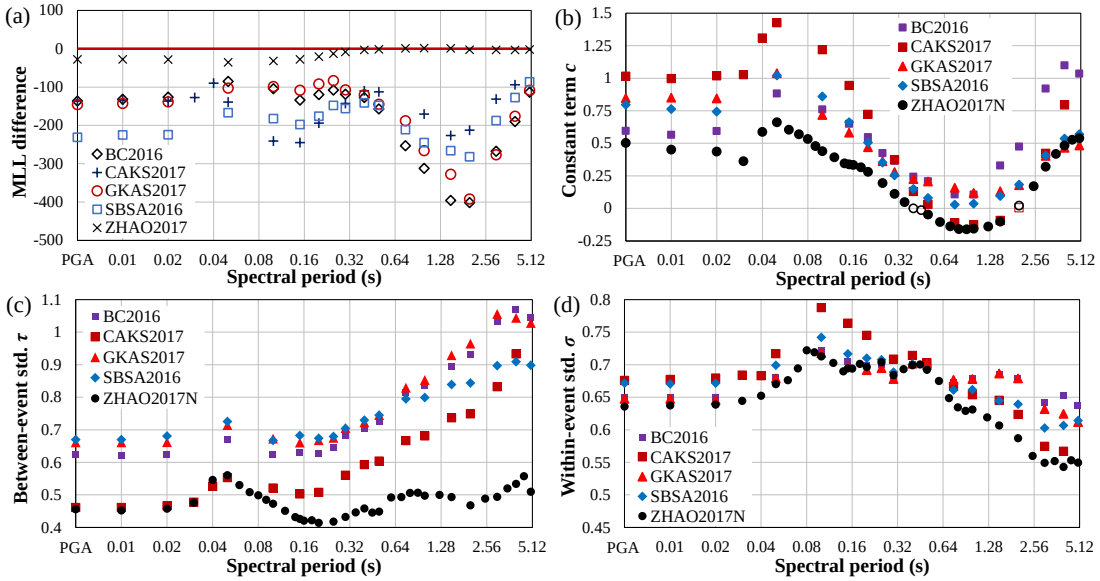

Figure 2 (a) The maximum log-likelihood increase, (b) the constants for five GMPEs, (c) the between-event and (d) the within-event standard deviations for five GMPEs.

To compare the MML values, we normalized the MML for each GMPE, i.e., subtracting the MLL of the ZHAO2017N from that of each GMPE. For a given GMPE, if the MLL difference is positive, this GMPE may have a better performance than the ZHAO2017N, and if the difference is negative the GMPE is likely to have overall performance worse than that of ZHAO2017N model. Figure 2(a) suggests that the MLL values from all GMPEs are less than those of the ZHAO2017N and the largest negative value is about 400 from the BC2016 and GKAS2017 models. The normal fault term from the Zhao et al [5] leads to a slightly reduced MLL at short periods. Figure 2 (b) presents the constant correction term c in Equation (1). This term reflects the overall model performance. The smaller this term the better the GMPE for the SWC dataset. At spectral periods up to 0.5s and over 2.0s the values for the ZHAO2017N model are the smallest among the five GMPEs. At short periods up to 0.2s, c for the CAKS2017 model is the largest, and c for the BC2016 model is the largest at spectral periods over 1.5s. At the spectral period range of 0.5-2.0s, the values from the ZHAO2017N are similar

to those from the other GMPEs. Figure 2(c) compares the between-event standard deviation τ from Equation (1) and the ZHAO2017N model has the smallest values at nearly all spectral periods, suggesting that this GMPE model depicts the source effect of the SWC dataset to the best extents among these GMPEs. At spectral periods up to 0.5s, the between-event standard deviations for the NGA-West2 models have similar values, varying between 0.62 and 0.75. Starting at 0.6s, the between-event standard deviations for the NGA-West2 models increase with increasing spectral periods, to a peak value of about 1.07 at 4.0s. The CAKS2017 model has similar τ values to those from the ZHAO2017N model at short periods up to 0.07s. At longer periods, the between-event standard deviations of the CAKS2017 model increase with increasing spectral periods and are in parallel to the curves of GKAS2017 and the BC2016 models. The between-event standard deviations of the CAKS2017 model are largely between those of the NGA-West2 models and those of the ZHAO2017N model, about 0.15 less than those of the NGA-West2 models. For the within-event standard deviations labeled by σ presented in Figure 2(d), the ZHAO2017N model has the smallest σ values at nearly all periods. The CAKS2017 model has the largest values at spectral periods up to 0.5s. Three NGA-West2 models have reasonably similar values at nearly all spectral periods with the largest difference being about 0.05.

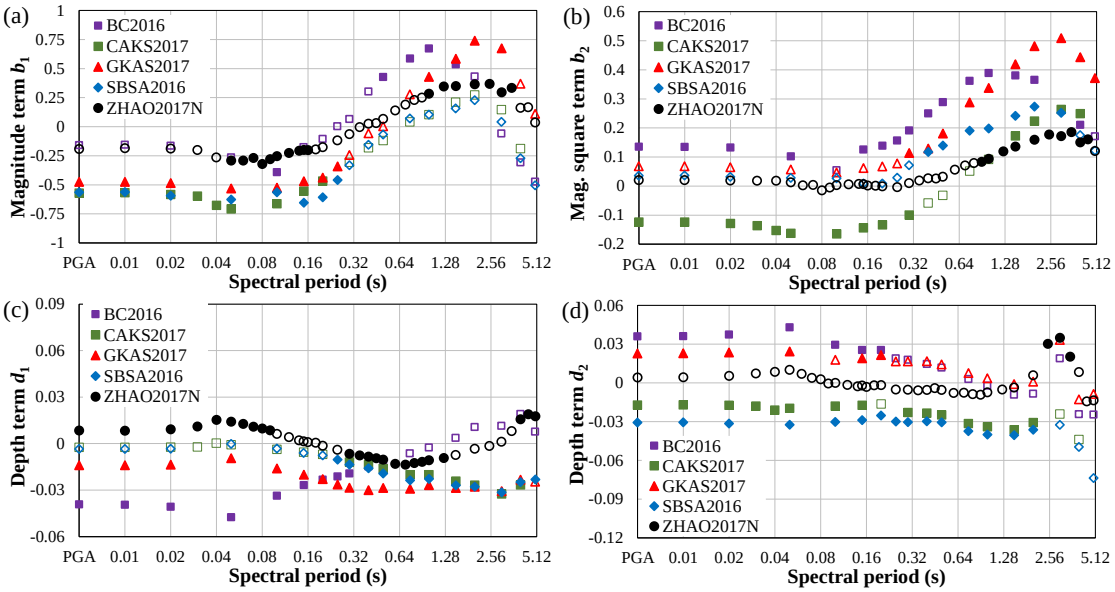

Figure 3 The correction coefficients for (a) the magnitude term and (b) the magnitude squared term, (c) the first depth term and (d) the second depth term for five GMPEs.

The correction coefficients for the linear magnitude term are presented in Figure 3(a) and for the magnitude squared term in Figure 3(b). The unfilled symbol means that this coefficient is not statistically larger than 0.0 at a significance level of 5%. At the spectral period up to 0.2s, the values from the ZHAO2017N and BC2016 models are very similar, varying between -0.32 and -0.11 and are not statistically significant at many spectral periods. The values of linear magnitude term b_1 for the BC2016 model are the largest in the spectral period range of 0.2s – 1.0s and the GKAS2017 model has the largest values at periods over 1.5s. At spectral periods up to 0.5s, the CAKS2017, GKAS2017, and SBSA2016 models have similar but large negative values. At long periods over 3.0s, the values of b_1 for the BC2016, CAKS2017, and SBSA2016 models are similar but with large negative values. However, these values are not all statistically significant, suggesting that the associated standard deviation is large. Figure 3(b) shows that, at spectral periods up to 0.7s, b_2 for the ZHAO2017N model has very small values that are not statistically significant, and at spectral periods over 1.25s, b_2 for this model has the smallest values among all GMPEs. The magnitude squared term for the CAKS2017 model has the largest negative values at spectral periods up to 0.3s and this term for the BC2016 model has the largest values at spectral periods up to 1.0s and is statistically significant. At spectral periods over 1.5s, the values for b_2 from the GKAS2017 model has the largest values and are statistically significant.

These results suggest that nearly all GMPEs require corrections for the magnitude effect terms in this long period range. Figure 3(c) presents the coefficients for the depth correction terms. Overall the first depth term d_1 from the ZHAO2017N model has the smallest variation range of -0.014 and 0.019. At short periods up to 0.15s, depth correction terms d_1 for the CAKS2017 and SBSA2016 models have the smallest absolute values. The correction term for the BC2016 model has the largest negative values at short periods up to 0.15s and the values for the ZHAO2017N model are reasonably close to 0.0 but are statistically larger than 0.0 at many spectral periods. At spectral periods over 0.2s, the depth correction term d_1 from GKAS2017 has the largest negative values close to -0.03. Figure 3(d) suggests that the correction coefficient d_2 for the ZHAO2017N model is not statistically significant and has the smallest absolute values for nearly all spectral periods among the five models. The BC2016 model has the largest correction values at most periods whereas the SBSA2016 model has the largest negative values at most spectral periods. The differences among the NGA-West2 models are considerable, varying in a range of -0.03-0.03.

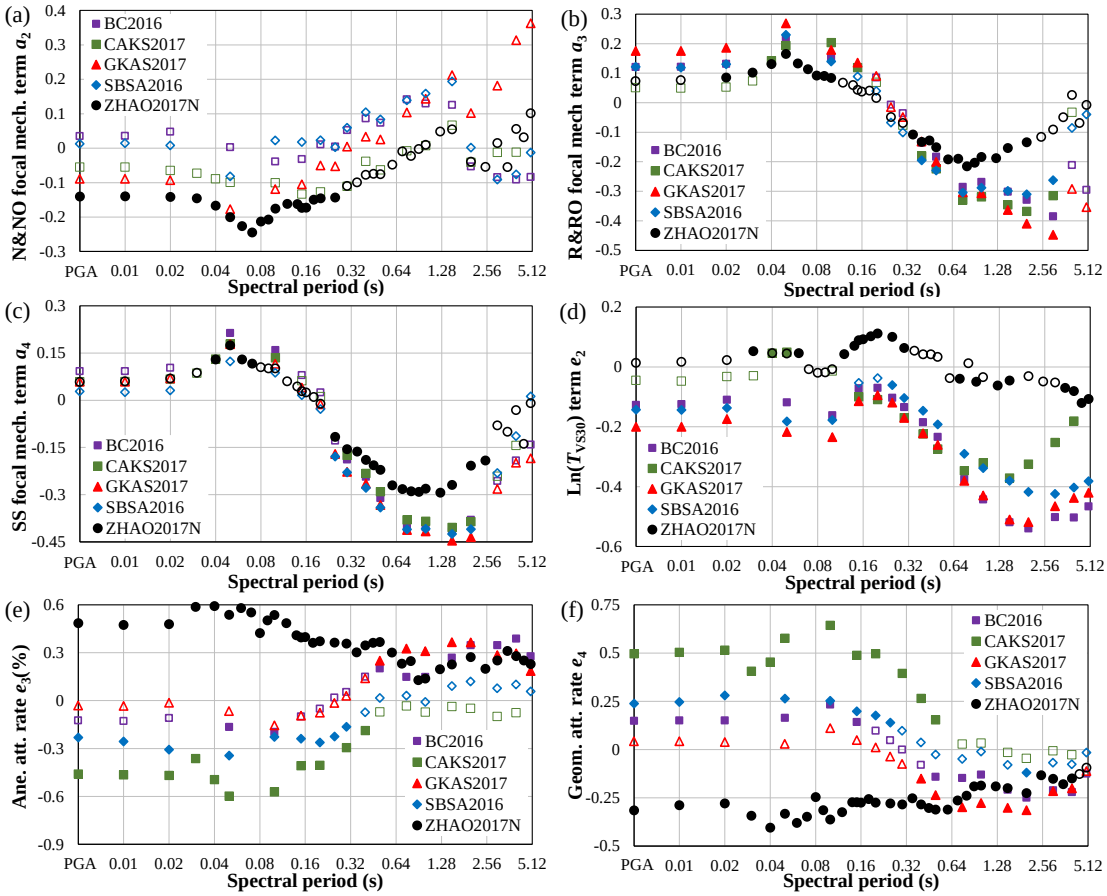

Figure 4 The correction coefficients for (a) normal fault events, (b) reverse fault events and (c) strike-slip events, (d) the site effect term, (e) the anelastic attenuation term, and (f) geometric attenuation term for five GMPEs.

Figure 4 presents the correction coefficients for focal mechanism group, anelastic attenuation and geometric attenuation terms. Figure 4(a) suggests that the correction coefficients for the N&NO term from the ZHAO2017N model have the largest negative values and are statistically significant at short periods up to 0.3s whereas the coefficients are not statistically significant at other spectral periods. The coefficients from the other four models are largely not statistically significant at all spectral periods. Figures 4(b) and 4(c) show that the ZHAO2017N model generally requires the smallest absolute values for the correction coefficients for both R&RO and SS focal mechanism groups at many spectral periods. At short spectral periods, the correction coefficients from all models are relatively small, and at periods over 0.5s the correction coefficients have large

negative values, suggesting that the spectra from the R&RO and SS events in the SWC dataset are overestimated significantly by all models tested in this study. The correction coefficients for the SS events are similar to those of the R&RO events, suggesting that these two types of focal mechanisms can be combined at one group of events for developing a GMPE for the SWC dataset. Figure 4(d) shows that the correction coefficient for the site effect calculated from the between-site residuals for the ZHAO2017N model has the smallest absolute values among the five GMPEs, varying between -0.12 and 0.11. The correction coefficients from the other GMPEs all have negative values and the largest negative value is about -0.54 for the BC2016 model and -0.52 for the GKAS2017 model at a spectral period of 2.0s. Figure 4(e) shows that the correction coefficients for the anelastic attenuation term. For short periods, the distance correction coefficients from the ZHAO2017N model are positive and vary between 0.0013 and 0.0059. The total values, i.e. the combined values of the correction coefficients with the anelastic attenuation rates from this GMPE, are negative for all spectral periods. The correction coefficients from the BC2016 and GKAS2017 models are very close to zero and are not statistically significant at short periods up to 0.3s. The correction coefficients from the CAKS2017 model have large negative values with the largest one being -0.006. The large negative coefficients are a possible result of the zero anelastic attenuation rate for this GMPE. At short periods up to 0.3s, the SBSA2016 model has a moderate correction coefficient value of -0.003 at short periods up to 0.3s. At spectral periods over 0.5s, the correction coefficients for BC2016 and GKAS2017 are close to 0.003. Note that the additional attenuation terms for China in the NGA-West2 models were accounted for in the calculation of correction coefficients. The adjusted anelastic attenuation rates using a small number of the strong-motion record from the SWC region may not produce uniform improvement. The SBSA2016 model, for example, still requires a considerable correction coefficient with a value of close to -0.003 at short periods up to about 0.3s, whereas the BC2016 and GKAS2017 GMPEs require a correction coefficient for anelastic attenuation with a value up to 0.004 at periods over 0.6s. Figure 4(f) presents the correction coefficients for the geometric attenuation terms. At short periods up to 0.2s, the correction coefficients for the GKAS2017 model are very close to zero and those for the other two NGA-West2 models are close to 0.25. The correction coefficients for the ZHAO2017N model vary between -0.4 and -0.09 and are statistically significant at all spectral periods except for 4.5 and 5.0s. The CAKS2017 model requires very large correction coefficients at spectral periods up to 0.4s whereas the coefficients are not statistically significant at spectral periods over 0.5s. The largest correction coefficient for this GMPE is 0.64.

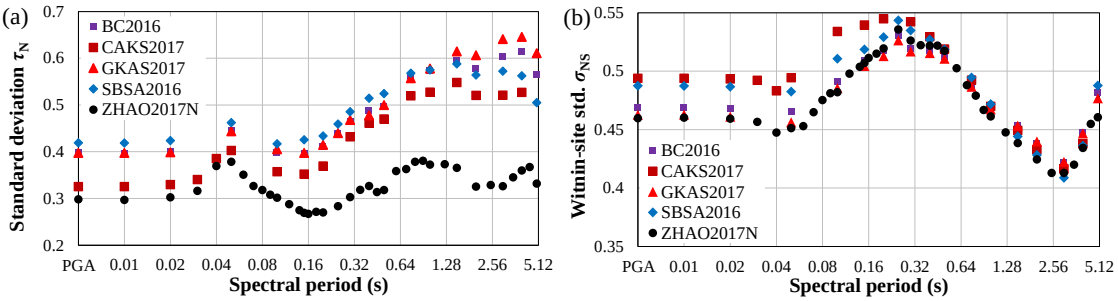

Figure 5 (a) The between-event and (b) the within-site standard deviations after the correction functions were applied.

The standard deviation τ_N from Equation (5) is equivalent to the between-event standard deviation when the corrections in Equation (5) applied to each GMPEs though this is not a mathematically sound assumption. For the purpose of model comparison, τ_N can be used as a goodness-of-fit indicator. The smaller τ_N is, the better the model fits the dataset. Figure 5(a) shows that the ZHAO2017N model has the smallest values for τ_N, varying between 0.28 and 0.38, significantly less than the standard deviations from all other models, especially at spectral periods over 0.1s. The CAKS2017 model has the second-smallest values τ_N at all periods, varying between 0.33 for PGA and 0.53 at a spectral period of 5.0s. The standard deviations for the three NGA-West2 models are similar at periods up to about 1.0s and the differences at long periods are considerable, with the largest difference is just over 0.1. Note that the between-event standard deviations of the SWC dataset cannot be reduced to the same value for all GMPEs when a correction function with physically-based model

parameters in Equation (5) was used. This means that, before developing a new GMPE, it would be useful to select an appropriate GMPE by model comparison similar to the approaches presented in this study and that by the Lan et al. [8] study.

The between-site standard deviation τ_{NS} from Equation (6) and τ_{NS} would be close to the between-site standard deviation for a random effects model fitted to the SWC dataset. The values for τ_{NS} from these GMPEs (not presented in this article) are very similar, if not identical, at all periods varying between 0.15 and 0.53. These results suggested that the between-site standard deviations from all GMPEs plus the simple correction functions in Equation (6) can be similar in the site response modeling for all GMPEs. Figure 5(b) presents the within-site standard deviations. In contrast to the between-site standard deviations, the within-site standard deviation differ moderately among the five GMPEs at spectral periods up to 0.3s. The values for σ_{NS} from the CAKS2017 model are larger than those from the other GMPEs with the largest difference being about 0.05 only. At spectral periods over 0.3s, the values for σ_{NS} from all GMPEs are very similar. The σ_{NS} from the ZHAO2017N model is either close to or less than those from the other GMPEs across all periods.

4. Aftershock effect

The GKAS2017 model has an aftershock term and the BC2016 model did not use the aftershock records in the NGA-West2 dataset; the CAKS2017, SBSA2016 and ZHAO2017N models used the aftershock data without an aftershock term. If the aftershock effect is significant in the SWC dataset, the GKAS2017 GMPE would model the mainshock and aftershock data equally well and the BC2016 GMPE would model the mainshocks better than aftershocks. We calculated the average values for γ_i in Equation (4) for the main and aftershocks and these average values can be used as a plausible indicator whether the ground motions from the aftershocks differ from those of the mainshocks.

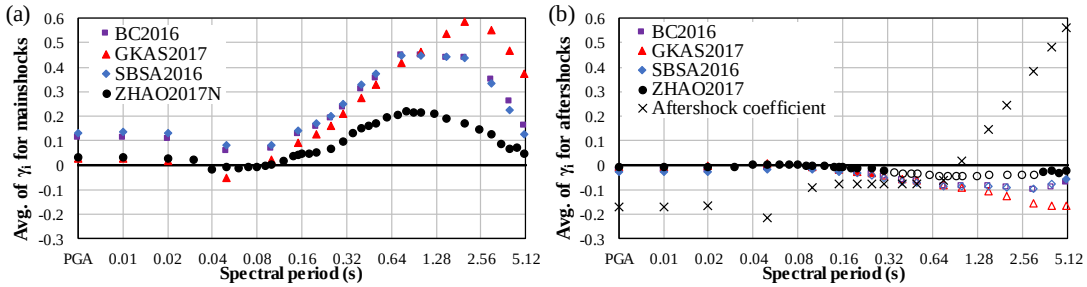

Figure 6 Mean between-event residuals for (a) the mainshocks and (b) the aftershocks for four GMPEs.

Figure 6(a) presents the average mainshock residuals and a common feature is that the ZHAO2017N model has the smallest values at most spectral periods. The variation pattern of the average mainshock residual is that the average mainshock residuals are generally small at short periods up to about 0.2s, increases with increasing period to a peak value and then decrease with increasing period. At short periods up to 0.1s, the average mainshock residuals for the GKAS2017 and the ZHAO2017N models are close to 0.0, whereas the average mainshock residuals for the BC2016 and the SBSA2016 models are close to about 0.1 at short periods. At the other spectral periods, the residuals from these two GMPEs are very similar even though the BC2016 model did not use the aftershock records and the SBSA2016 model used the aftershock data without an aftershock term. We would expect that the average mainshock residuals from the BC2016 model should be smaller than that from the SBSA2016 model because mainshocks would be better modeled by the BC2016 GMPE. The average mainshock residuals from the GKAS2017 model are close to zero at very short periods up to 0.1s and this may be the result of using the aftershock term in this GMPE. However, the averaged residuals at moderate and long periods are larger. The large values of the average mainshock residuals at long periods are probably from the biased distribution of the mainshock data for which the bias with respect one model parameter cannot be averaged out for another parameter, because of the relatively small number of mainshocks and the small number of records. Figure 6(b) presents the average aftershock residuals from four GMPEs and the aftershock terms in the GKAS2017 GMPE. The average between-event residuals for the

aftershocks for all models are close to zero at short spectral periods up to about 0.2s and become negative at about 0.15s. The average residuals decrease with increasing periods at periods over 0.15s. At periods over 0.3s, the average aftershock residuals are not statistically significant. The average aftershock residuals from all GMPEs are not similar to the aftershock terms from the GKAS2017 model. In summary, it is fair to conclude that the aftershock effect cannot be modeled well or is not significant for the vertical component of the SWC dataset.

5. Ranking the GMPEs for the SWC dataset

In this study, we evaluated the correction functions with coefficients based on a simple function of the physical parameters, such as magnitude, fault depth, attenuation rate, and site response. If the coefficient for a given term is zero or not statistically significant, this term from the corresponding GMPE can be considered to be suitable for the SWC dataset. Intuitively, if a correction coefficient for a GMPE has the smallest absolute value it would be plausible to consider this GMPE as the best to model the physical part associated with this model parameter. Following Lan et al. [8], if a GMPE will be modified and used with or without modification for the SWC dataset, the following GMPE ranking criteria may be considered. For an ideal case, this GMPE should have:

1) the largest MLL for separating the total residuals into a constant, between- and within-event residuals Equation (1);

2) the smallest absolute values for constant c in Equation (1);

3) the smallest between-event standard deviations τ for the between-event residuals η_i and the smallest within-event standard deviations σ for the within-event residuals $\xi_{i,j}$ defined in Equation (1);

4) the smallest absolute values for the added magnitude scaling rates b_1 and b_2, depth scaling rates d_1 and d_2, site effect term e_2, anelastic attenuation rate e_3, and geometric attenuation rate e_4 in Equation (6); and

5) the smallest between-event standard deviations τ_N from Equation (5) and within-event standard deviations σ_N from Equation (6), after the source and path correction terms are applied.

Table 1 GMPE ranking

	Const. c	σ	τ	b_1	b_2	d_1	d_2	e_2	e_3	e_4	τ_N	Avg.
GKAS2017	3	4	1	1	2	1	4	1	4	4	1	2.36
BC2016	2	2	2	4	1	2	3	2	3	3	3	2.45
CAKS2017	1	1	4	2	3	4	2	4	2	1	4	2.55
SBSA2016	4	3	3	3	4	3	1	3	5	5	2	3.27
ZHAO2017N	5	5	5	5	5	5	5	5	1	2	5	4.36

Because none of the GMPEs evaluated in this study would satisfy these requirements at all spectral periods, Lan et al. [8] designed a simple and informal (in terms of statistical analyses) scheme to evaluate the performance of these GMPEs for the horizontal component of the SWC dataset. Firstly, if the MLL derived from Equation (1a) is used as a ranking criterion, the average MLL values across 18 spectral periods would lead the following ranking order for these GMPEs: ZHAO2017N, CAKS2017, BC2016, GKAS2017, and SBSA2016. The largest MLL difference among the three NGA-West2 GMPEs is relatively small and the difference between the ZHAO2017N model and the other four models is relatively large. Next, we calculated the average of the absolute values for constant c and added model parameters b_1, b_2, d_1, d_2, e_2, e_3, and e_4, the between- and within-event standard deviations across 18 spectral periods for each of the 5 GMPEs. Coefficients a_1 in Equation (3) and e_1 in Equation (6) were not used as part of a goodness-of-fit parameter because they are not independent parameters in each of the two equations. We decided to exclude MLL from the ranking comparison in Table 1 because MLL contains the same information in the between- and within-event standard deviations (a large MLL will lead to small standard deviations). We excluded τ_{NS} and σ_{NS} as

ranking variables because the differences in τ_{NS} and σ_{NS} among all models in a wide period band are very small. When a variable for one model is very close to that from another model, a rank difference of 1.0 for the two model does not reflect the real differences of two models. We also excluded the variables for focal mechanisms because many earthquakes in our dataset do not have one. The ranks of these GMPEs were assigned according to the average absolute values for each parameter with 5 being for the model with the smallest average values and 1 for the model with the largest average absolute values of these parameters, as shown in Table 1. Among the five models, the ZHAO2017N GMPE has the largest average ranking index in Table 1 and may be considered to be the best GMPE for the SWC dataset with or without modification.

Table 1 shows that the ZHAO2017N model has the largest ranking index of 4.36 and the SBSA2016 model has the second-largest ranking index of 3.27. If we include a_2, a_3, and a_4, the coefficients for focal mechanisms, the rank for the ZHAO2017 model is unchanged because the absolute values for these coefficients for the ZHAO2017 model are the smallest among the five GMPEs at many spectral periods.

6. Conclusions

We compared the vertical response spectra of the strong-motion dataset recorded in the Western and the Southwestern part of China (referred to as the SWC region). We used a dataset of 2403 high-quality digital strong-motion records from 449 earthquakes among which only 73 are mainshocks. There is a large magnitude gap in the dataset; for example, there is only one event between M_W 6.3 and M_W 7.8. Among 449 events 259 events do not have a known focal mechanism. The average number of records per event or per site is small. The reliable site condition parameters such as V_{S30} are available only for some stations. These shortcomings reduce the statistical powers of the dataset and make it difficult to develop a reliable GMPE without external data or without appropriate functional form from GMPEs developed from a large dataset with desirable event and date distributions. In this study, we carried out a detailed comparison of the SWC dataset with three GMPEs by Bozorgnia and Campbell [1] (BC2016), Gülerce et al. [2] (GKAS2017), Stewart et al. (2016) [3], developed from the NGA-West2 dataset, a GMPE by Çağnan et al. [4] based on the Europe and the Middle East dataset (CAKS2017), and a GMPE by Zhao et al. [5] (ZHAO2017N disregarding the normal fault term) based on the strong-motion records from the shallow crustal and upper mantle events in Japan. A constant term was first used to scale the GMPEs to match the SWC dataset and the residuals were separated into the between- and within-event parts using a random effects regression method. A set of correction functions were built with terms based on source, path and site effects and the absolute values of the regression coefficients were used to rank these GMPEs. The smaller the absolute values for the correction coefficients, the better for this GMPE to match the SWC dataset. The following conclusions can be reached.

1) The overall goodness-of-fit parameters such as the constant correction term (c in Equation (1) that can be used to scale a GMPE) and the maximum log-likelihood (MLL) can be used to rank these GMPEs. The MLL values lead to the following ranking orders from the best to the worst: the ZHAO2017N, CAKS2017, BC2016, GKAS2017, and SBSA2016. The ranking numbers for the three GMPEs based on the NGA-West2 dataset are reasonably similar. If the correction coefficients for the focal mechanism were used, the ranking order is largely the same;

2) We tested the aftershock effect. The GKAS2017 model has an aftershock term and the BC2016 model did not use the aftershock records in the NGA-West2 dataset; the other three GMPEs used the aftershock data without an aftershock term. If the aftershock effect is significant in the SWC dataset, the GKAS2017 GMPE may model the mainshock and aftershock data equally well and the BC2016 GMPE may model the mainshock better than aftershocks. Our comparison does not suggest that the modeling of the aftershock effect would make a large difference, similar to conclusions reached by Lan et al. [8] for the horizontal component.

3) The between-event and within-event standard deviations for the SWC dataset calculated for different GMPEs vary significantly from one GMPE to another. The ZHAO2017 model appears to have the smallest standard deviations at nearly all spectral periods;

4) Statistically and practically significant correction coefficients for magnitude, fault depth, focal mechanism, path and site terms, were required for all GMPEs to match the SWC dataset. Generally, the

absolute values for many correction terms from the ZHAO2017 GMPE have the smallest absolute values at many spectral periods;

5) The between-event and within-site standard deviations from all models at many spectral periods cannot be reduced to the same values after correction functions were applied, whereas the between-site standard deviations are virtually the same for all GMPEs. The ZHAO2017N model has the smallest between-event standard deviation after the correction functions were applied;

6) The modeling of the aftershock does not make a significant difference.

7. Acknowledgments

The work reported here was partially supported by research grants from the National Science Foundation of China (51578470) and by the special grant from the Shandong Jianzhu University.

8. References

[1] Bozorgnia Y, Campbell KW (2016): Vertical ground motion model for PGA, PGV, and linear response spectra using the NGA-West2 database. *Earthquake Spectra*, **32** (2), 979–1004.

[2] Gülerce Z, Kamai R, Abrahamson NA, Silva WJ (2017): Ground motion prediction equations for the vertical ground motion component based on the NGA-W2 database. *Earthq. Spectra*, **33** (2), 499–528.

[3] Stewart JP, Boore DM, Seyhan E, Atkinson GM (2016): NGA-West2 equations for predicting vertical-component PGA, PGV, and 5%-damped PSA from shallow crustal earthquakes. *Earthq. Spectra*, **32** (2), 1005–1031.

[4] Çağnan Z, Akkar S, Kale Ö, Sandıkkaya A (2017): A model for predicting vertical component peak ground acceleration (PGA), peak ground velocity (PGV), and 5% damped pseudospectral acceleration (PSA) for Europe and the Middle East. *Bull. Earth. Eng.*, **15** (7), 2617–2643.

[5] Zhao JX, Jiang F, Ma Y, Zhou J, Cheng Y, Chang Z (2017): Ground-motion prediction equations for the vertical component from shallow crustal and upper-mantle earthquakes in Japan using site classes as the site term. *Bull. Seismol. Soc. Am.*, **107** (5), 2310–2327.

[6] Wooddell KE, Abrahamson NA (2014): Classification of main shocks and aftershocks in the NGA-West2 database. *Earthquake Spectra*, **30** (3), 1257–1267.

[7] Zhao JX, Zhou S, Zhou J, Zhao C, Zhang H, Zhang Y, Gao P, Lan X, Rhoades D, Fukushima Y, Somerville P.G., and Irikura K (2016): Ground-motion prediction equations for shallow crustal and upper-mantle earthquakes in Japan using site class and simple geometric attenuation functions. *Bull. Seismol. Soc. Am*, **106** (4), 1552-1569.

[8] Lan XW, Xing H, Zhou J, Zhao JX (2019): A comparison of the source, path, and site effects of the strong-motion records from the western and the southwestern parts of China with modern ground-motion prediction equations. *Bull. Seismol. Soc. Am*, **109** (6), 2691–2709.

[9] Abrahamson NA, Silva WJ (2008): Summary of the Abrahamson & Silva NGA ground-motion relations. *Earthq. Spectra*, 24(1), 67–97.

[10] Campbell KW, Bozorgnia Y (2008): NGA ground motion model for the geometric mean horizontal component of PGA, PGV, PGD and 5% damped linear elastic response spectra for periods ranging from 0.01 to 10 s. *Earthq. Spectra*, 24(1), 139-171.

[11] Abrahamson NA, Silva WJ, Kamai R (2014): Summary of the ASK14 ground motion relation for active crustal regions. *Earthq. Spectra*, **30** (3), 1025-1055.

[12] Campbell KW, Bozorgnia Y (2014): NGA-West2 ground motion model for the average horizontal components of PGA, PGV, and 5% damped linear acceleration response spectra. *Earthq. Spectra*, 30 (3), 1087-1115.

